Virology **254,** 213–219 (1999)
Article ID viro.1998.9555, available online at http://www.idealibrary.com on IDEAL®

RAPID COMMUNICATION

Influenza Virus Inhibits Cleavage of the HSP70 Pre-mRNAs at the Polyadenylation Site

Kazufumi Shimizu,[1] Akifumi Iguchi, Rieko Gomyou, and Yasushi Ono

Department of Microbiology, Nihon University School of Medicine, 30-1 Oyaguchikami-chou, Itabashi-ku, Tokyo 173-8610, Japan

Received September 2, 1998; returned to author for revision October 5, 1998; accepted November 30, 1998

Influenza virus infection is known to shut off the expression of host genes. To study the mechanism, we examined the effects of influenza A/Udorn/72 virus infection on the heat induction of a major heat shock protein, HSP70, in Madin–Darby canine kidney cells. The induction of HSP70 protein synthesis was progressively suppressed with postinfection time when heat shock was applied. Northern hybridization analysis revealed the appearance of longer, heterogeneous HSP70 transcripts in the range of 2.7 to 30 kb with a concomitant decrease in the amount of the mature 2.7-kb mRNAs in the nucleus of the infected cells. Such longer β-actin transcripts were also observed but with much less intensity. The longer HSP70 transcripts contained the downstream sequence of the polyadenylation site, as demonstrated by RNase protection with an antisense RNA probe containing the sequence through the polyadenylation sites. This clearly proved that influenza virus infection inhibits the polyadenylation-site cleavage of the pre-mRNAs by the host cleavage and polyadenylation machinery. One temperature-sensitive mutant virus carrying a temperature-sensitive mutation on the NS_1 gene failed to inhibit the cleavage at the nonpermissive temperature, indicating that the NS_1 protein is involved in the inhibition of the pre-mRNA cleavage. This is the first report of the down-regulation of cellular mRNA maturation at the point of polyadenylation-site cleavage by virus infection and identifies a new mechanism by which the influenza virus shuts off host gene expression.

Influenza is one of the major infectious diseases remaining to be controlled. The etiologic agent, influenza virus, is a unique RNA virus whose genome is composed of eight single-stranded RNA segments with negative polarity and is transcribed and replicated in the nucleus of infected cells (*1*), while most RNA viruses replicate in the cytoplasm. Infection with influenza virus results in a general decline in cellular protein synthesis, while there is an activation of several host genes related to host antiviral defense such as interferon-α/β, MxA, TNF-α, IL-1β, and IL-6 (*2, 3*). Two different mechanisms have been proposed to explain the shut-off of cellular protein synthesis during virus infection: degradation of preexisting cellular mRNAs (*4, 5*) and establishment of a virus-specific translational system (*6, 7*). Neither of the models, however, explains how viral and cellular mRNAs can be discriminated, because viral mRNAs have structural features similar to those of host mRNAs; the 5′ end sequences (10 to 13 nucleotides) of influenza mRNAs are snatched from host mRNAs and their 3′ ends have a poly(A) tail. The goal of this study is to examine the mechanism(s) underlying the influenza virus-induced shut-off of host gene expression. Here we focused on one specific inducible protein, a major heat shock protein, HSP70, to examine how influenza virus infection affects heat induction of the HSP70 protein.

The HSP70 protein is efficiently induced in Madin-Darby canine kidney (MDCK) cells by heat shock, i.e., raising the temperature from 34 to 40°C for 2 h, and the HSP70 protein band could be explicitly detected by one-dimensional SDS–polyacrylamide gel electrophoresis (Fig. 1, compare lane 1 with lane 2). In the MDCK cells infected with influenza A/Udorn/72 virus, the induction of HSP70 protein synthesis was progressively suppressed with postinfection time when heat shock was applied. In addition, many bands other than the HSP70 protein that were present in the mock-infected sample almost disappeared in the later heat induction (compare lanes 5 and 6 with lane 7). The suppression of these protein syntheses correlated with the increase in the synthesis of the viral proteins, thus demonstrating the shut-off of host protein synthesis.

We subsequently prepared RNAs separately from nuclear and cytoplasmic fractions at the same time points as in Fig. 1 and examined the HSP70 transcripts by Northern hybridization. The amount of mature HSP70 mRNAs of about 2.7 kb in size was increased upon the heat treatment of mock-infected cells, in both nucleus and cytoplasm (Fig. 2a, compare lanes 2 and 8 with lanes 1 and 7). In RNA samples prepared from the cytoplasm of

[1] To whom correspondence and reprint requests should be addressed. E-mail: kazu@med.nihon-u.ac.jp.

0042-6822/99 $30.00

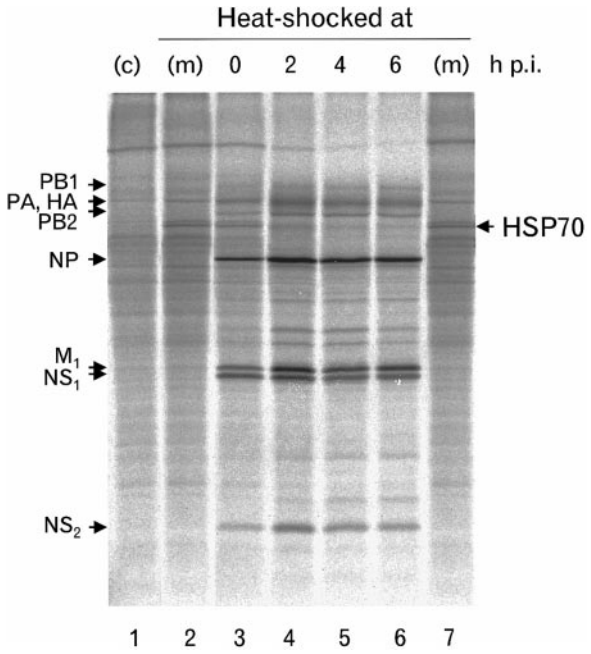

FIG. 1. Suppression of the induction of HSP70 expression in influenza virus-infected cells. MDCK cells were infected with influenza A/Udorn/72 wild-type virus at 34°C. The cells were heat-shocked (2-h duration at 40°C) at the indicated time postinfection (hpi) and pulse-labeled with [^{35}S]methionine for 30 min. The labeled proteins were electrophoresed on an 18% polyacrylamide gel containing 0.072% bisacrylamide, 0.1% SDS, and 3 M urea. The gel was fixed, dried, and visualized by a Fuji BAS2000 image analyzer (Fuji Photo Film Co., LTD.). c, mock-infection without heat shock; m, mock-infection with heat shock. The positions of viral proteins and HSP70 (confirmed by coelectrophoresis with the authentic protein immunoprecipitated by HSP70 specific antiserum) are indicated.

infected cells, the amount of mature 2.7-kb mRNAs decreased with heat shock time (lanes 9–12), agreeing with the suppression of HSP70 protein synthesis after virus infection. With RNAs prepared from the nuclear fraction we found an appearance of smears larger than the 2.7-kb band during infection, concomitant with a decrease in the intensity of the mature 2.7-kb bands (Fig. 2a, lanes 4, 5, and 6). The results indicated that the decrease in the mature 2.7-kb mRNAs in the cytoplasm was due to neither the degradation of HSP70 mRNA nor the inhibition of its nuclear export and also indicated that the virus infection did not block the HSP70 transcription per se, but did inhibit the normal maturation of the pre-mRNAs. The longer transcripts were heterogeneous in size, with the longest reaching approximately 30 kb. The majority of the longer transcripts did not seem to be polyadenylated, since they did not bind to oligo(dT)-conjugated beads (data not shown).

The blotted sheets used for the analysis of HSP70 transcripts were also hybridized with a β-actin probe. Faint smears larger than the 2.2-kb bands of mature β-actin mRNAs were detected in the nuclear RNAs from the infected cells (Fig. 2b, lanes 4, 5, and 6). In contrast to HSP70 mRNAs, mature β-actin mRNAs preexisted abundantly at the time of virus infection (Fig. 2b, lane 1) and the amount was not increased upon the heat treatment of mock-infected cells (lane 2). Thus, the majority of the transcripts detected in the infected cells represented preexisting transcripts; i.e., the transcripts that were synthesized after viral infection occupied a minor fraction. The faint smears, therefore, seemed to represent a significant portion of the newly synthesized transcripts and indicated that the virus infection inhibited the normal maturation of β-actin pre-mRNAs as well as HSP70 pre-mRNAs.

Because the MDCK HSP70 gene, like other eukaryotic HSP70 genes, contains no intron sequence, such an increase in the size of the transcripts should not be due to an inhibition of the splicing. Transcription of most eukaryotic protein genes terminates far downstream of the site where the mRNAs are polyadenylated. The primary transcripts are cleaved and polyadenylated at the site by a large complex of multisubunit proteins (cleavage and polyadenylation complex) (*8, 9*). It seemed possible, therefore, that the longer HSP70 transcripts in the

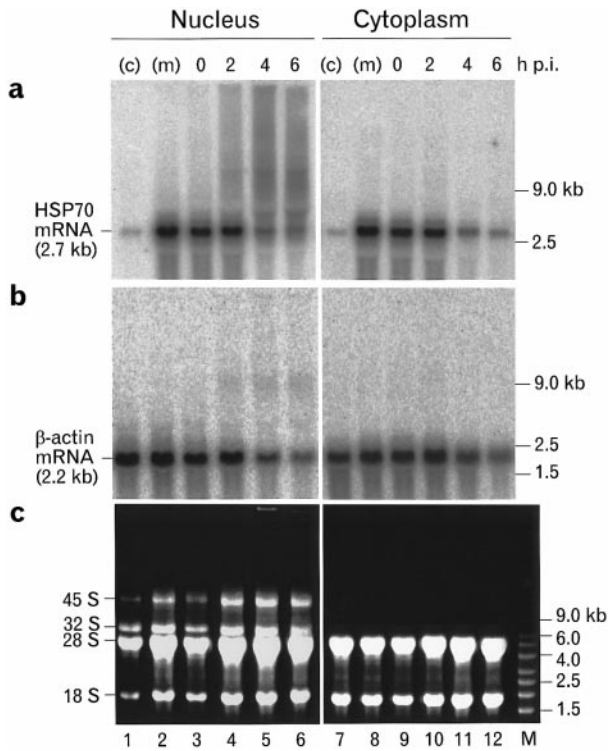

FIG. 2. Northern hybridization of HSP70 transcripts. The infected cells were exposed to heat shock at the same time intervals as in Fig. 1 and fractionated into nucleus and cytoplasm. RNA from each fraction was subjected to Northern blot analysis using a ^{32}P-labeled antisense probe of HSP70 mRNA (a) and β-actin mRNA (b). The ethidium bromide staining (c) shows that the 45S and 32S ribosomal RNA precursors are present solely in the nuclear fraction and not in the cytoplasmic fraction, indicating a successful fractionation of nucleus and cytoplasm without appreciable RNA degradation. Lane M, 2-μg RNA size markers (Millennium, Ambion, Inc.).

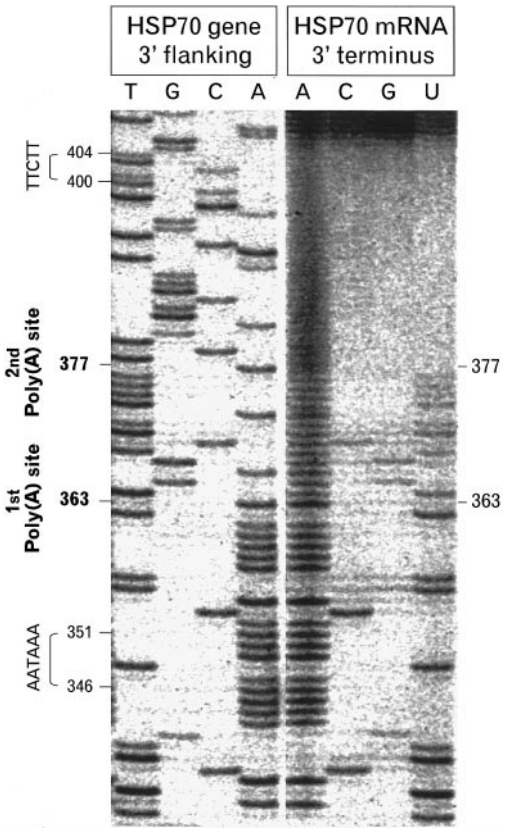

FIG. 3. Determination of HSP70 mRNA poly(A) sites. The genomic sequence of the 3′ flanking region of the MDCK HSP70 gene and the 3′ terminal sequence of the mRNA were compared in a sequencing gel. The nucleotide numbers are indicated on both sides; they start from the A next to the stop codon and continue downstream. The genome sequence and the mRNA sequence coincide until A363, from which major mRNAs are polyadenylated. A subset of mRNAs contains the genome sequence beyond A363 up to A377, where its polyadenylation starts.

nucleus of infected cells were pre-mRNAs without the endonucleolytic cleavage at the polyadenylation site. We tested this possibility by RNase protection assay using an antisense probe that contains the sequence through the cleavage and polyadenylation site. For this purpose, we first amplified a DNA fragment that contained the 3′-flanking region of the HSP70 gene of MDCK cells and determined its nucleotide sequence. The consensus sequence (AATAAA) of the polyadenylation signal (*10*) was found 346 nucleotides downstream of the stop codon, and the downstream consensus U-rich element (TTCTT) (*11*) was found 400 nucleotides downstream. In Fig. 3, the sequence of the cDNA from the HSP70 mRNA was compared with that of the genomic DNA. The intensities of the sequence bands of the cDNA were high until A363 (for the nucleotide number, see the legend to Fig. 3), above which they abruptly became low except for those of the A ladder. The low-density bands continued until A377, above which no bands other than As were observed. These results indicate that polyadenylation starts at two sites: the first major site was at 12 bases (A363), and the second minor site was at 26 bases (A377), downstream of the polyadenylation signal (see Fig. 4a).

We then prepared an RNA probe complementary to the sense strand from C419 to T230 through the two cleavage and polyadenylation sites (for the numbering of the bases of the sense strand, see the legend to Fig. 3; this numbering is also employed for the bases of the antisense strand; see Fig. 4a). This antisense probe had 196 bases including 6 extra bases. In RNase T1 protection experiments using the probe, the protected fragments of 139 and 149 nucleotides (nt) were expected for the HSP70 transcripts cleaved and polyadenylated at the first and the second sites, respectively (see the legend to Fig. 4a), while the fragment of 191 nt (full length) was expected for the uncleaved read-through transcripts. Both the nuclear and the cytoplasmic RNAs from heat-treated mock-infected cells yielded mainly the 139- and 149-nt cleaved fragments (Fig. 4b, lanes 3 and 9). The nuclear RNAs from infected cells showed a decrease in the cleaved probe fragments and an increase in the 191-nt uncleaved probe fragments as the virus infection proceeded (Fig. 4b, lanes 4–7). This result indicates that influenza virus infection results in the inhibition of cleavage at the two cleavage and polyadenylation sites. The cytoplasmic RNAs from the same infected cells showed a decrease in both cleaved and uncleaved fragments, indicating that the nuclear uncleaved transcripts were not exported into the cytoplasm (lanes 12 and 13). Faint smears larger than the 2.7-kb band of mature HSP70 mRNA were detected in both the nuclear and the cytoplasmic RNAs from the mock-infected cells after heat shock by Northern hybridization assay (Fig. 2, lanes 2 and 8). These seemed to be polyadenylated as they were transported to the cytoplasm. A minor portion of the HSP70 transcripts (10–20%; deduced from the intensities of signals) was considered to be cleaved and polyadenylated, not at the first and second polyadenylation sites we identified, but at random sites downstream. All the mRNAs polyadenylated after G419 (see Fig. 4a) could yield the protected fragments of 191 bases. Thus the 191-base bands appeared with the cytoplasmic RNAs (Fig. 4b, lanes 9–13). The bands decreased with the infection time, indicating that the cleavage and polyadenylation at the random sites are also inhibited by the virus infection. The increased 191-base bands with the nuclear RNAs in virus-infected cells represented the uncleaved transcripts that were not polyadenylated and, therefore, not exported to the cytoplasm.

To identify which virus-encoded gene product is involved in the above inhibition of pre-mRNA cleavage, we made use of various temperature-sensitive (*ts*) mutants of A/Udorn/72 (H3N2) virus (*12*). The temperature of the HSP70 heat induction (40°C for 2 h) is the nonpermissive temperature for the ts mutants. Their permissive temperature is 34°C and the HSP70 protein was induced by a

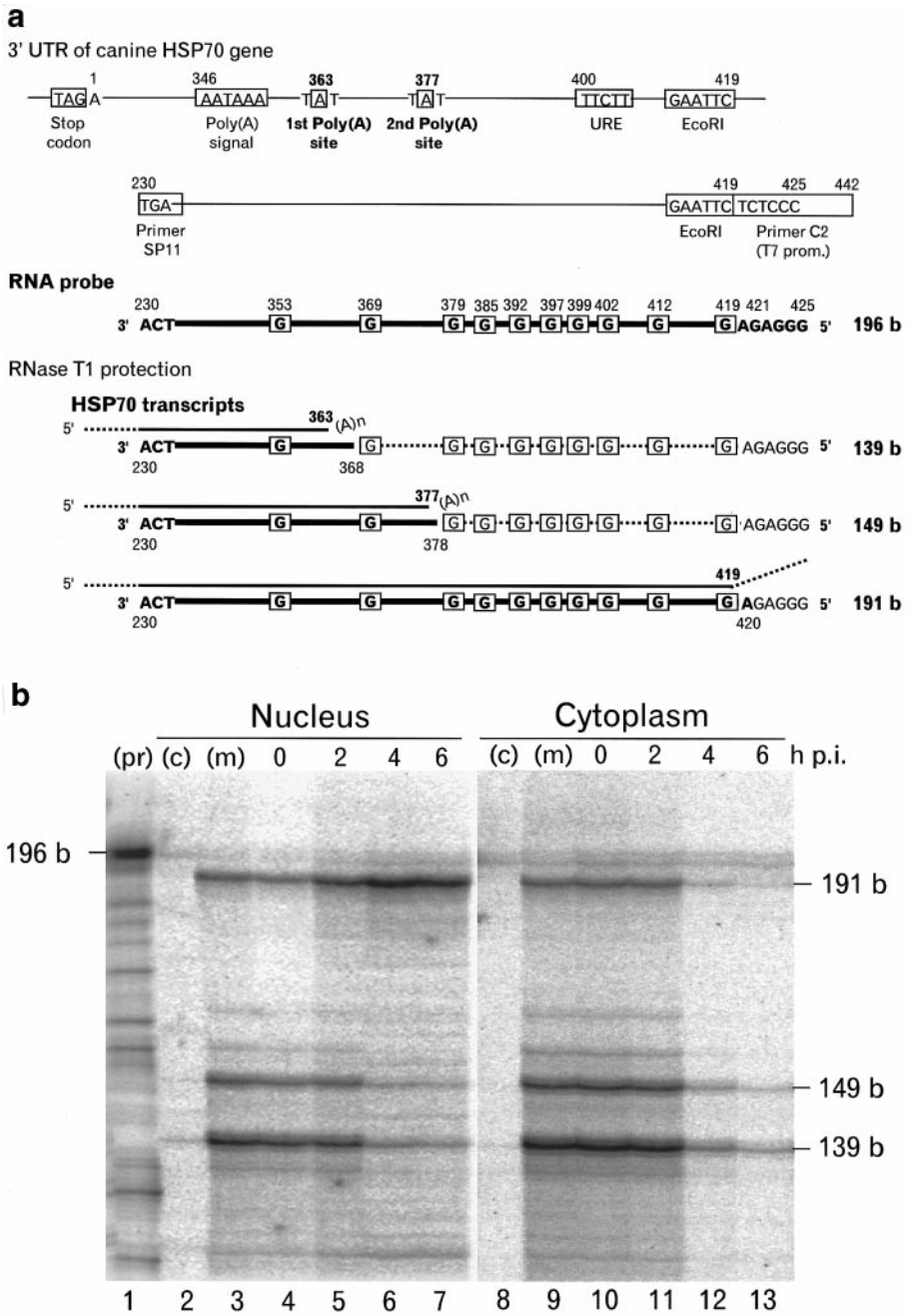

FIG. 4. Inhibition of the cleavage at the polyadenylation sites of HSP70 pre-mRNAs by influenza virus infection. (a) Scheme of RNase T1 protection assay. The sites susceptible to RNase T1 digestion (the 3′ phosphate groups of guanine nucleotides) in the region downstream of the poly(A) signal are indicated by Gs with the position number. For the first (or second) site cleavage and polyadenylation, the unprotected Gs are G369 (or G379) and those positioned toward the 5′ end of the probe providing the 139-base (or 149-base) fragment, while for the uncleaved transcripts at the both sites, they are G421 and those positioned toward the 5′ end providing the 191-base fragment. (b) RNase T1 protection assay. The same RNA samples as for Fig. 2 were subjected to the assay. Lane 1, 0.1 fmol undigested probe (pr). The positions of the fragments protected by the cleaved transcripts (139 and 149 bases) and uncleaved transcripts (191 bases) are indicated.

2-h incubation at 34°C in the presence of 50 μM sodium arsenite. One of the mutants, ICR452, which carries a *ts* lesion on the NS genome RNA segment shown by complementation assay (*13*), exhibited distinct temperature-sensitivity in the inhibition of HSP70 induction. The induction of HSP70 protein synthesis was severely suppressed at 34°C but not at 40°C in ICR452-infected cells (Fig. 5a, compare lanes 3 and 4 with lanes 1 and 2), while it was suppressed at both 34 and 40°C in wild-type virus-infected cells (lanes 5 and 6). Northern hybridization analyses of HSP70 transcripts in nuclei revealed that the majority of the transcripts were pre-mRNAs with sizes longer than the mature mRNA of 2.7 kb in ICR452-infected cells at 34°C but the majority at 40°C were

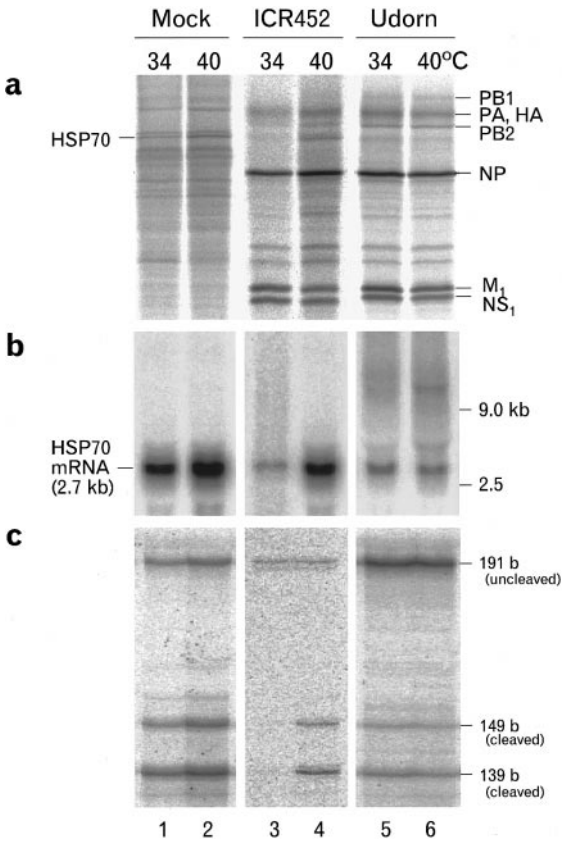

FIG. 5. Temperature-sensitive suppression of the induction of HSP70 expression in ICR452-infected cells. MDCK cells were infected with ICR452 (one of the NS_1 *ts* mutants of influenza A/Udorn/72 virus) or with the wild-type virus (Udorn) or mock-infected (Mock) for 4 h at 34°C. Then cells were treated for HSP70 induction at the permissive temperature of 34°C for 2 h in the presence of 50 μM sodium arsenite or at the nonpermissive temperature of 40°C for 2 h. (a) Protein synthesis was analyzed as described in the legend to Fig. 1. (b) HSP70 transcripts in the nuclear fractions were analyzed by Northern hybridization. (c) The cleavage of HSP70 pre-mRNAs at the polyadenylation sites was analyzed by RNase T1 protection assay of HSP70 transcripts in the nuclear fractions. The positions of the fragments protected by the cleaved transcripts (139 and 149 bases) and uncleaved transcripts (191 bases) are indicated.

mature mRNAs (Fig. 5b, lanes 3 and 4). The majority in wild-type virus-infected cells were longer pre-mRNAs at both 34 and 40°C (lanes 5 and 6) and in mock-infected cells mature mRNAs were found at both temperatures (lanes 1 and 2). The cleavage of HSP70 pre-mRNAs at the polyadenylation sites was inhibited at 34°C in ICR452-infected cells but not at 40°C (Fig. 5c, compare lanes 3 and 4 with lanes 1 and 2), while it was inhibited at both 34 and 40°C in wild-type virus-infected cells (lanes 5 and 6). To identify the mutation responsible for the temperature-sensitivity, the nucleotide sequence of the ICR452 NS genome segment was determined. Two base substitutions were observed, one of which, a C to U transition at base 62, causes no change in the amino acid residue. The other, an A to G transition at base 316, causes an amino acid change of Glu to Gly at residue 96 of the NS_1 protein. This occurs between two previously identified functional domains of the NS_1 protein (*14*): the RNA binding domain (amino acids 19–38) and the effector domain (amino acids 134–161). These results indicated that a function of the NS_1 protein is required for the inhibition of cleavage at the polyadenylation sites of the pre-mRNAs.

The results presented above proved that HSP70 mRNA maturation was suppressed in the influenza virus-infected cells at the stage of endonucleolytic cleavage at the polyadenylation sites catalyzed by the cellular cleavage and polyadenylation complex. The NS_1 protein of the virus was shown to be involved in inhibiting the cleavage reaction. It seems likely that the inhibition of mRNA maturation is not restricted to the HSP70 pre-mRNAs, but occurs more generally with other pre-mRNAs. In evidence of this, we observed that the maturation of the pre-mRNAs for β-actin was also inhibited in influenza virus-infected cells (Fig. 2b). The uncleaved transcripts, however, occupied a minor fraction because the mature mRNAs for such house-keeping genes preexist abundantly at the time of virus infection. Thus the stability of the mRNAs may be the major determinant in the shut-off of the synthesis of preexisting proteins.

Since the viral mRNAs do not have the same consensus polyadenylation signal as animal cells (AAUAAA), the cellular enzyme complex that functions in the cleavage and polyadenylation of pre-mRNAs is not thought to be involved in the polyadenylation of the viral mRNAs, for which a mechanism of reiterative copying of a U-stretch by the viral transcription complex has been proposed ("slippage" or "stuttering" model) (*15, 16*). This differential mechanism may explain the selective inhibition of cellular mRNA maturation in the virus infection. It should be noted, however, that at the late phase of infection when the inhibition mechanism is established, synthesis of all the viral mRNAs declines dramatically, whereas synthesis of the vRNAs reaches its maximum (*17*). The inhibition of the cleavage of pre-mRNAs at the polyadenylation site, therefore, seems to be kinetically coupled with the increase in vRNA synthesis and the decrease of viral mRNA synthesis. It is possible that the host pre-mRNA cleavage and the viral vRNA synthesis compete for a common resource in the virus-infected cells and the NS_1 protein plays a role in the competition. It was recently shown that influenza virus NS_1 protein interacts with the cellular 30-kDa subunit of the cleavage and polyadenylation specificity factor (CPSF), which is an essential component of the mammalian pre-mRNA 3′ end processing machinery, and binding of the NS_1 protein to the 30-kDa protein inhibits 3′ end cleavage and polyadenylation of pre-mRNAs that are transcribed from transfected artificial DNAs (*18*). This is in good agreement with our results obtained with natural cellular mRNAs.

The shut-off mechanism of mRNA maturation is expected to work most efficiently at suppressing the cellu-

lar genes that are induced during viral infection. Despite this, some cellular genes are activated, exerting antiviral functions (*3*) after the virus infection. The dynamics of the shut-off and the activation of cellular genes during virus growth may be crucial in determining the outcome of infection not only at the cellular level (from abortive to productive and cytolytic infection) but also at the clinical level (from asymptomatic to fatal infection), which is the subject of further studies.

Madin–Darby canine kidney cells were cultivated in MEM containing 10% fetal bovine serum at 34°C. The confluent monolayer cells were used in all experiments. Cells were infected at 34°C with influenza A/Udorn/307/72 (H3N2) virus or ICR452, one of the *ts* mutants derived from the Udorn wild-type virus (*13*), at multiplicity of infection of 5 after 1 h of adsorption at room temperature. To induce the HSP70 protein synthesis the infected cells were either heat-shocked for 2 h at 40°C or incubated for 2 h in the presence of 50 μM sodium arsenite (a potent chemical inducer of heat shock proteins) at 34°C.

The MDCK cells on an 8-cm plate were scraped off, lysed in 0.3 ml of 0.5% Nonidet-P40 in 50 mM Tris–HCl (pH 7.4), 100 mM KCl, 5 mM magnesium acetate at 0°C, and centrifuged at 5000 rpm for 5 min in a microcentrifuge. The pellet was used as the nuclear fraction and the supernatant as the cytoplasmic fraction. RNAs were dissociated from proteins by the addition of guanidinium thiocyanate solution (4 M guanidinium thiocyanate, 25 mM sodium citrate (pH 7), 0.1 M 2-mercaptoethanol, 0.5% *N*-lauroylsarcosine) up to 0.9 ml and preferentially precipitated in 25% (v/v) ethanol as described (*19*). The RNA pellets collected by centrifugation were dissolved in 50 μl of TE buffer. DNA was, when necessary, recovered from the supernatant by precipitation in 50% ethanol. The DNA pellet was dissolved in 500 μl of TE buffer.

Two microliters of RNA was denatured in 50% formamide and 17.5% formalin, mixed with 0.5 μg ethidium bromide for prestaining at 60°C for 5 min, and electrophoresed on a 1% agarose gel containing 3% formalin. The ethidium bromide-staining profile was photographed to monitor the quantity and intactness of ribosomal RNAs. Then the RNAs were blotted onto a nitrocellulose filter (Hybond-N, Amersham International plc) with 0.05 M NaOH. The ^{32}P-labeled antisense probe was prepared by asymmetrical PCR amplification of a coding region of the canine HSP70 gene (from nucleotides 220 to 2 to the stop codon) or β-actin (from nucleotides 673 to 829 of the coding region). The blot was visualized with a Fuji BAS2000 image analyzer.

cDNAs of cytoplasmic mRNAs of heat-shocked, mock-infected MDCK cells were synthesized using a T-Primed First-Strand Kit (Pharmacia Biotech). A part of the coding sequence near the stop codon of canine HSP70 gene was then amplified from the cDNAs by two rounds of PCR using nested primers that were designed to amplify a 219-bp fragment based on the conserved sequences of eukaryotic HSP70 genes (*20*). The sequence of PCR products was determined using a Takara *Taq* Cycle Sequencing Kit (Takara Shuzo Co., Ltd.).

The *Eco*RI cassette library was constructed by ligation of an *Eco*RI cassette (Takara Shuzo Co., Ltd.) to *Eco*RI-digested genomic DNA of MDCK cells. Using the cassette library as a template, a DNA fragment of 619 bp that contained the 3′ flanking region of the HSP70 gene was amplified by two rounds of PCR using nested primer sets (two sense primers, designated 3p and 5p, which were derived from the sequence of the 3′ coding region of the HSP70 gene; and two cassette primers C1 and C2 (antisense primers), whose sequences are contained in the *Eco*RI cassette). The fragment contained the 578-bp sequence of the HSP70 gene, 159 bases from the 3′end of the HSP70 coding region continuing through the stop codon (TAG) to 419 bases downstream (the sequence was deposited with the DNA Data Bank of Japan, under Accession No. AB013075).

A sense primer, 9p, was designed to amplify the sequence of bases 34–419 downstream from the stop codon using the cassette primer C2 as an antisense primer. The 3′ untranslated region of MDCK HSP70 mRNA was amplified from its cDNAs by two rounds of PCR using seminested primer sets (two sense primers, 5p and 9p, and one antisense primer, *Not*I–$(dT)_{18}$). The amplified fragments were sequenced by direct PCR sequencing using primer 11p, which has the sequence of bases 230–249 from the stop codon, and the sequences obtained were compared with the genomic sequence of the 3′ flanking region.

The radioactive antisense probe that is complementary to the sequence from the position 230 to 419 bases downstream from the HSP70 stop codon (Fig. 4a) was synthesized by T7 polymerase in the presence of [α^{32}P]UTP and the PCR-amplified fragment as the template, which was produced using 11p and C2 primers and contained the T7 promoter sequence in antisense primer C2. The RNA sample of 2.5 μl (equivalent to RNAs in 5×10^5 cells) was hybridized to the probe (10 fmol) and subjected to RNase T1 digestion. One-half of the final material was loaded onto a 6% acrylamide gel containing 7 M urea. Gels were dried and visualized with a Fuji BAS2000 image analyzer.

Viruses were grown and purified as previously described (*12*). RNAs were extracted as described above. cDNAs of the virus genome RNAs were synthesized using a You-Primed First-Strand Kit (Pharmacia Biotech) and amplified by PCR using common primers that were designed to amplify all genome cDNAs based on the 3′- and 5′-terminal common sequences of all the genome segments. The NS genome cDNAs were amplified by second-round PCR using the terminal common primers and NS-specific inner primers. The sequence of the PCR

products was determined using a Takara *Taq* Cycle Sequencing Kit (Takara Shuzo Co., Ltd.).

ACKNOWLEDGMENTS

We thank H. Ohmori, R. Fukuda, and B. R. Murphy for critically reading the manuscript and for discussions; N. Shimizu and T. Tahira for technical help and advice; K. Kamata for cDNA sequencing; H. Nakamura for reagents; and M. Yamaki for his continuous support. This work was supported in part by a Grant-in-Aid for Scientific Research from the Ministry of Education, Science and Culture of Japan (07670352).

REFERENCES

1. Lamb, R. F., and Krug, R. M. (1996). Orthomyxoviridae: The viruses and their replication. *In* "Fields Virology" (B. N. Fields, D. M. Knipe, and P. M. Howley, Eds.), 3rd ed., pp. 1353–1395. Lippincott-Raven, Philadelphia.
2. Peschke, T., Bender, A., Nain, M., and Gemsa, D. (1993). Role of macrophage cytokines in influenza A virus infections. *Immunobiology* **189,** 340–355.
3. Ronni, T., Matikainen, S., Sareneva, T., Melén, K., Pirhonen, J., Keskinen, P., and Julkunen, I. (1997). Regulation of IFN-α/β, MxA, 2′,5′-oligoadenylate synthetase, and HLA gene expression in influenza A-infected human lung epithelial cells. *J. Immunol.* **158,** 2363–2374.
4. Inglis, S. C. (1982). Inhibition of host protein synthesis and degradation of cellular mRNAs during infection by influenza and herpes simplex virus. *Mol. Cell. Biol.* **2,** 1644–1648.
5. Beloso, A., Martinez, C., Valcárcel, J., Santarén, J. F., and Ortin, J. (1992). Degradation of cellular mRNA during influenza virus infection: Its possible role in protein synthesis shutoff. *J. Gen. Virol.* **73,** 575–581.
6. Kate, M. G., and Krug, R. M. (1984). Metabolism and expression of RNA polymerase II transcripts in influenza virus-infected cells. *Mol. Cell. Biol.* **4,** 2198–2206.
7. Feigenblum, D., and Schneider, R. J. (1993). Modification of eukaryotic initiation factor 4F during infection by influenza virus. *J. Virol.* **67,** 3027–3035.
8. Wahle, E., and Keller, W. (1996). The biochemistry of polyadenylation. *Trends Biochem. Sci.* **21,** 247–250.
9. Colgan, D. F., and Manley, J. L. (1997). Mechanism and regulation of mRNA polyadenylation. *Genes Dev.* **11,** 2755–2766.
10. Proudfoot, N. J., and Brownlee, G. G. (1976). 3′ Non-coding region sequences in eukaryotic messenger RNA. *Nature* **263,** 211–214.
11. Chen, F., MacDonald, C. C., and Wilusz, J. (1995). Cleavage site determinants in the mammalian polyadenylation signal. *Nucleic Acids Res.* **23,** 2614–2620.
12. Shimizu, K., Mullinix, M. R., Chanock, R. M., and Murphy, B. R. (1982). Temperature-sensitive mutants of influenza A/Udorn/72 (H3N2) virus. II. Genetic analysis and demonstration of intrasegmental complementation. *Virology* **117,** 44–61.
13. Shimizu, K., Mullinix, M. R., Chanock, R. M., and Murphy, B. R. (1983). Temperature-sensitive mutants of influenza A/Udorn/72 (H3N2) virus. III. Genetic analysis of temperature-dependent host range mutants. *Virology* **124,** 35–44.
14. Qian, X.-Y., Alonson-Caplen, F. V., and Krug, R. M. (1994). Two functional domains of the influenza virus NS1 protein are required for regulation of nuclear export of mRNA. *J. Virol.* **68,** 2433–2441.
15. Luo, G., Luytjes, W., Enami, M., and Palese, P. (1991). The polyadenylation signal of influenza virus RNA involves a stretch of uridines followed by the RNA duplex of the panhandle structure. *J. Virol.* **65,** 2861–2867.
16. Pritlove, D. C., Poon, L. L., Fodor, E., Sharps, J., and Brownlee, G. G. (1998). Polyadenylation of influenza virus mRNA transcribed *in vitro* from model virion RNA templates: Requirement for 5′ conserved sequences. *J. Virol.* **72,** 1280–1286.
17. Shapiro, G. I., Gurney, T., Jr., and Krug, R. M. (1987). Influenza virus gene expression: Control mechanisms at early and late times of infection and nuclear-cytoplasmic transport of virus-specific RNAs. *J. Virol.* **61,** 764–773.
18. Nemeroff, M. E., Barabino, S. M. L., Li, Y., Keller, W., and Krug, R. M. (1998). Influenza virus NS_1 protein interacts with the cellular 30 kDa subunit of CPSF and inhibits 3′ end formation of cellular pre-mRNAs. *Mol. Cell* **1,** 991–1000.
19. Siebert, P. D., and Chenchik, A. (1993) Modified acid guanidinium thiocyanate–phenol–chloroform RNA extraction method which greatly reduces DNA contamination. *Nucleic Acids Res.* **21,** 2019–2020.
20. Hunt, C., and Morimoto, R. I. (1985). Conserved features of eukaryotic *hsp70* genes revealed by comparison with the nucleotide sequence of human hsp70. *Proc. Natl. Acad. Sci. USA* **82,** 6455–6459.